



TITLE:

C-13 nuclear Overhauser polarization
nuclear magnetic resonance in rotating
solids: Replacement of cross polarization in
uniformly C-13 labeled molecules with
methyl groups

AUTHOR(S):

Takegoshi, K; Terao, T

CITATION:

Takegoshi, K ...[et al]. C-13 nuclear Overhauser polarization nuclear magnetic resonance in rotating solids: Replacement of cross polarization in uniformly C-13 labeled molecules with methyl groups. JOURNAL OF CHEMICAL PHYSICS 2002, 117(4): 1700-1707

ISSUE DATE:

2002-07-22

URL:

<http://hdl.handle.net/2433/49978>

RIGHT:

Copyright 2002 American Institute of Physics. This article may be downloaded for personal use only. Any other use requires prior permission of the author and the American Institute of Physics.

^{13}C nuclear Overhauser polarization nuclear magnetic resonance in rotating solids: Replacement of cross polarization in uniformly ^{13}C labeled molecules with methyl groups

K. Takegoshi and Takehiko Terao

Department of Chemistry, Graduate School of Science, Kyoto University, Kyoto 606-8502, Japan

(Received 21 March 2002; accepted 22 April 2002)

A new ^{13}C polarization technique in solids is presented on the basis of a recently proposed ^{13}C – ^{13}C recoupling sequence [^{13}C – ^1H dipolar-assisted rotational resonance (DARR), K. Takegoshi, S. Nakamura, and T. Terao, *Chem. Phys. Lett.* **344**, 631 (2001)] operative under fast magic angle spinning (MAS), in which a rf field is applied to ^1H with a rotary resonance condition but none to ^{13}C . The ^1H irradiation in DARR saturates ^1H signals, leading to the ^{13}C signal enhancement due to the nuclear Overhauser effect for fast rotating methyl groups, if any. If we use a uniformly ^{13}C labeled sample, ^{13}C – ^{13}C polarization transfer enhanced by DARR successively distributes the enhanced methyl carbon polarization to the other ^{13}C spins, leading to uniform enhancement for all ^{13}C spins even under very fast MAS. In uniformly ^{13}C labeled rotating samples, the enhancement factor in cross polarization (CP) is about 2.4, while in the present nuclear Overhauser polarization (NOP), it is 3.0 in the fast rotation limit of the methyl groups. While the CP enhancement becomes smaller for molecules with short $T_{1\rho}$ of ^1H or ^{13}C , NOP would work well for such mobile molecules, and also NOP enables us to acquire a signal with a short repetition time even if ^1H T_1 is long. Further, NOP has the advantage of quantitiveness, and is very easy to carry out, being insensitive to the adjustment of rf field intensity and requiring only very low rf power. These features are demonstrated for uniformly ^{13}C , ^{15}N -labeled *L*-threonine and uniformly ^{13}C , ^{15}N -labeled glycylisoleucine. NOP-MAS is also applied for a naturally abundant ^{13}C sample.

© 2002 American Institute of Physics. [DOI: 10.1063/1.1485062]

I. INTRODUCTION

Cross polarization (CP) is a prerequisite technique for improving the sensitivity in solid-state NMR of dilute and/or low γ spins (*S*).^{1,2} CP enables us to acquire a signal with a repetition time of the spin-lattice relaxation time (T_1) of the abundant ^1H spins (*I*), which is usually much shorter than those of the *S* spins. CP also enhances the magnetization of the *S* spins with a low gyromagnetic ratio by $\sim \gamma_I/\gamma_S$ compared to the thermal equilibrium value. However, as will be pointed out below, this advantage of CP becomes less appealing for multiply/uniformly ^{13}C -labeled samples. In this work, we examined the possibility of replacing CP by a polarization technique based on the nuclear Overhauser effect (NOE).³

In liquid NMR of low γ spins, NOE has widely been used to achieve a short repetition time and signal enhancement.^{4,5} NOE is brought about by rf irradiation capable of saturating ^1H spins dipolar coupled to the observed spins. Cross relaxation in the coupled spin system under rf irradiation leads the spin system into a quasiequilibrium state in which the signal intensities are enhanced appreciably. In contrast to the popularity of NOE in liquid NMR, however, application of NOE in high-resolution NMR in solids has not been fully examined yet. This is ascribed to the NOE mechanism unfavorable for rigid molecules. For efficient NOE, (i) the spin to be enhanced should relax dominantly by the fluctuation of the dipolar interaction with the spin under rf irra-

diation, and further, (ii) the correlation time of the motion responsible for the dipolar fluctuation should be smaller than the inverse of the Larmor frequency of the irradiated spin. Both conditions are fulfilled for molecules in liquid, however, condition (ii) in particular is not realized for solid molecules in general. Some exceptional examples are found in mobile rubbery polymers.⁶ For a rigid solid, it is envisaged that NOE would be appreciable for molecules with fast internal motion. In fact, Naito *et al.* examined the spin-lattice relaxation of ^{13}C spins in *L*-alanine with or without ^1H rf irradiation, and found an appreciable NOE signal enhancement for the CH_3 carbon.⁷ This is reasonable because ^{13}C relaxation in solids is dominated by the ^{13}C – ^1H dipolar coupling, and the CH_3 group rotates rapidly around the C– CH_3 bond.

Recently, we developed a novel ^{13}C – ^{13}C polarization transfer method [^{13}C – ^1H dipolar-assisted rotational resonance (DARR)].⁸ In DARR, the ^{13}C – ^1H dipolar interaction is recovered by the ^1H rf irradiation with intensity ν_1 satisfying the rotary-resonance condition $\nu_1 = n\nu_{\text{MAS}}$ ($n = 1$ or 2),⁹ where ν_{MAS} is the spinning frequency. The spectral overlap between the two relevant ^{13}C spins, which is required for efficient polarization transfer based on rotational resonance,^{10–12} is realized between a spinning sideband of one ^{13}C spin and the ^{13}C – ^1H dipolar pattern of the other ^{13}C spin and vice versa. In the present work, we examined the possibility of achieving NOE and enhancing the signals of all rigid carbons by DARR. Since we applied rf to ^1H spins in

DARR, NOE enhancement would occur for ¹³C spins in fast rotating groups such as CH₃. The enhanced polarization is then successively transferred by DARR to the other ¹³C, leading to overall NOE enhancement even for stationary ¹³C. For the latter purpose, however, DARR may not be optimal, because it was shown that DARR recoupling occurs band-selectively between carboxyl/carbonyl/aromatic carbons and aliphatic carbons.⁸ We recently found that in the second order, recoupling does occur among ¹³C resonances with smaller chemical shift differences, such as aliphatic carbons. Although its efficiency is not very high, it is still appreciable for a long recoupling time. Theoretical details will be published elsewhere. Experimentally, it will be shown below that the recoupling occurs nonselectively for a recoupling time of a few seconds. We refer to this method of enhancing signal intensities by NOE and DARR as nuclear Overhauser polarization (NOP).

II. EXPERIMENT

Uniformly ¹³C, ¹⁵N-labeled *L*-threonine (Thr) was purchased from Cambridge Isotope Laboratories, Inc. and used without purification. Uniformly ¹³C, ¹⁵N-labeled glycylisoleucine (Gly-Ile) was prepared as described previously.¹³ The NMR experiments on Thr and Gly-Ile were carried out using a Chemagnetics CMX-400 spectrometer operating at the resonance frequency of 100.3 MHz for ¹³C with a CP/MAS probe (Chemagnetics) for a 3.2 mm rotor. Both of the MAS frequency ν_{MAS} and the ¹H rf intensity ν_1 for DARR were 20 kHz. The TPPM decoupling¹⁴ was used with the nutation angle and the phase-modulation angle being optimized for a rf intensity of 100 kHz to be 180° and ±15°, respectively. The NMR experiments on nonlabeled dimedone (5,5-dimethyl-1,3-cyclohexanedione) were done using a Chemagnetics CMX-300 spectrometer operating at the resonance frequency of 75.6 MHz for ¹³C with a CP/MAS probe (Doty Sci., Inc.) for a 5 mm rotor. Both of the MAS frequency and the DARR rf intensity were 10 kHz, and the CW ¹³C–¹H decoupling was adopted with an intensity of ≈80 kHz.

For CP enhancement at $\nu_{\text{MAS}} = 20$ kHz, the ¹H rf intensity was 50 kHz and the ¹³C rf intensity was varied linearly from 68 to 72 kHz with the contact time divided into 10 segments during each of which the ¹³C rf intensity was kept constant. The signal enhancement based on NOP was examined as follows: Prior to ¹H irradiation, three 90° pulses were applied to ¹³C with an interval of 10 ms to remove ¹³C longitudinal magnetization. Then a ¹H rf field is applied for a certain NOP time, and the resultant magnetization is observed under ¹H decoupling. The ¹H rf-field strength for NOP was set to satisfy the DARR condition ($\nu_1 = \nu_{\text{MAS}}$). The ¹³C spin-lattice relaxation curves were observed using the Torchia's pulse sequence.¹⁵

III. THEORY

First, we compare the possible enhancement factors for CP and NOE. The enhancement factor of CP is given by^{1,2}

$$\eta_{\text{CP}} = \frac{\gamma_I}{\gamma_S} \frac{N_I}{N_I + N_S}, \quad (1)$$

where N_I and N_S are the numbers of *I* and *S* spins, respectively. The average proton to carbon ratio N_I/N_S is calculated to be 1.65 for the 20 standard amino-acid residues in a peptide, leading to the theoretical maximum gain of ≈2.4 for a fully ¹³C-labeled peptide. For a dipolar coupled two-spin (*I*–*S*) system, Solomon derived simultaneous differential equations,¹⁶ which was further extended to a system with a dilute *S* spin in abundant *I* spins having a common spin temperature.¹⁷ Under the steady-state condition with ¹H saturation, the NOE factor can formally be written as

$$\xi_{\text{NOE}} = \frac{\gamma_I}{\gamma_S} \frac{6J(\omega_I + \omega_S) - J(\omega_I - \omega_S)}{J(\omega_I - \omega_S) + 3J(\omega_S) + 6J(\omega_I + \omega_S)}, \quad (2)$$

where $J(\omega)$ is a spectral density function, and ω_X is the Larmor frequency of the *X* spin. For a rotating methyl group, Naito *et al.* have deduced an apparent form of $J(\omega)$;⁷ however, the following form is sufficient for evaluation of ξ_{NOE} :

$$J(\omega) \propto \frac{\tau_r}{1 + \omega^2 \tau_r^2}, \quad (3)$$

where τ_r is the rotational correlation time τ of the CH₃ group. Note here that the overall signal intensity for ¹³C becomes $1 + \xi_{\text{NOE}}$ times of that obtained at thermal equilibrium and we define the NOE enhancement factor η_{NOE} as $1 + \xi_{\text{NOE}}$ to compare directly with η_{CP} . The enhancement reaches the maximum,

$$\eta_{\text{NOE}} = 1 + \frac{1}{2} \frac{\gamma_I}{\gamma_S}, \quad (4)$$

at the extreme narrowing limit of relaxation, i.e., $J(\omega) \sim \tau_r$. For *I*=¹H and *S*=¹³C, this becomes ca. 3.0. Hence, the maximum intensity possibly achieved by NOP is somewhat better than that by CP for fully ¹³C-labeled peptides.

The polarization created for ¹³CH₃ is then distributed to the other ¹³C spins by DARR recoupling. To incorporate the ¹³C spins coupled to ¹³CH₃ in the calculation, we consider a spin system consisting of N L_i (¹³C) spins ($i=1, \dots, N$) coupled to the *S* (¹³C) spin of a rotating CH₃ group. For simplicity, we assume that there is no cross relaxation between the ¹H spins of the CH₃ group (*I*) and the L_i spins. Similar to the assumption made by Brooks *et al.*,¹⁷ the other ¹H spins are assumed to have the common spin temperature and are not apparently included. In other words, we assume that only the ¹³C spin of the CH₃ group is enhanced by NOE due to the CH₃ protons. Experimentally, however, we found the direct NOE takes place for ¹³C spins in close proximity to CH₃ groups as will be shown below. Here we would like to examine effects of the presence of the other ¹³C spins to η_{NOP} quantitatively.

The simultaneous differential equations describing the time dependence of the magnetizations are written as

$$\frac{d\langle I_Z \rangle}{dt} = -\frac{1}{T_1} (\langle I_Z \rangle - I_0) - \frac{1}{T_1^{\text{IS}}} (\langle S_Z \rangle - S_0) - R \langle I_Z \rangle, \quad (5)$$

$$\frac{d\langle S_Z \rangle}{dt} = -\frac{1}{T_1^S}(\langle S_Z \rangle - S_0) - \frac{1}{T_1^{ST}}(\langle I_Z \rangle - I_0) - \sum_{i=1}^N k_i(\langle S_Z \rangle - \langle L_{iZ} \rangle), \quad (6)$$

$$\frac{d\langle L_{iZ} \rangle}{dt} = -\frac{1}{T_1^{L_i}}(\langle L_{iZ} \rangle - L_0) - k_i(\langle L_{iZ} \rangle - \langle S_Z \rangle), \quad (7)$$

where k_i is the polarization transfer rate between S and L_i , T_1^X is the spin-lattice relaxation time of the X spin, T_1^{XY} is the cross relaxation time between the X and Y spins, and X_0 denotes the thermal-equilibrium magnetization of the X spin. The last term in Eq. (5) represents the saturation effect due to ^1H rf irradiation. We further assume that the polarization transfer rates for the L_i spins are equal ($k_i = k$) and also the relaxation time ($T_1^{L_i} = T_1^L$). When ^1H is saturated ($R \gg 1/T_1^I, 1/T_1^{IS}$ and thus $\langle I_Z \rangle = 0$) and the system reaches the internal equilibrium, we have

$$\begin{aligned} \langle S_Z \rangle_{\text{eq}} &= \left\{ 1 + \frac{1 + kT_1^L}{1 + k(T_1^L + NT_1^S)} \xi_{\text{NOE}} \right\} S_0 \\ &\equiv \eta_{\text{NOP}}^S S_0, \\ \langle L_Z \rangle_{\text{eq}} &= \left\{ 1 + \frac{kT_1^L}{1 + k(T_1^L + NT_1^S)} \xi_{\text{NOE}} \right\} L_0 \\ &\equiv \eta_{\text{NOP}}^L L_0, \end{aligned} \quad (8)$$

where $\langle L_Z \rangle$ is the average of the z magnetization of the L_i magnetizations $\langle L_Z \rangle = (1/N) \sum_i \langle L_{iZ} \rangle$, η_{NOP}^X is the NOP enhancement factor for the X spin, and we used the relation,¹⁶

$$\xi_{\text{NOE}} = \frac{T_1^S}{T_1^{SI}} \frac{I_0}{S_0}, \quad (9)$$

which is identical to Eq. (2) when the relaxation times are governed by the ^{13}C – ^1H dipolar fluctuation. Note that for the slow polarization transfer limit $k \sim 0$, the NOP enhancement factor for the S spin is identical to the NOE enhancement factor $\eta_{\text{NOE}} = 1 + \xi_{\text{NOE}}$, while that for the L spin is $\eta_{\text{NOP}}^L = 1$. On the other hand, at the fast transfer limit ($kT_1^L \gg 1, kNT_1^S$), both NOP enhancement factors become equal to be η_{NOE} . At the intermediate region, Eq. (8) indicates a reduced enhancement factor for η_{NOP}^S as compared to η_{NOE} due to the presence of the L spins and further the NOP enhancement factor for the L spins is smaller than that for the S spin.

IV. RESULTS AND DISCUSSION

First, better enhancement by NOP is demonstrated for a powder sample of uniformly ^{13}C , ^{15}N -labeled L -threonine (Thr). Figure 1 shows the ^{13}C MAS spectra obtained for Thr using a single 90° pulse without NOP (a), with NOP (b), and using CP (c). 64 FIDs were accumulated for each experiment, and the spectra in Fig. 1 are plotted on the same amplitude scale and can be directly compared. For the single 90° pulse experiment with NOP [Fig. 1(b)], the NOP time was 10 s with the ^1H rf-intensity fulfilling the DARR condi-

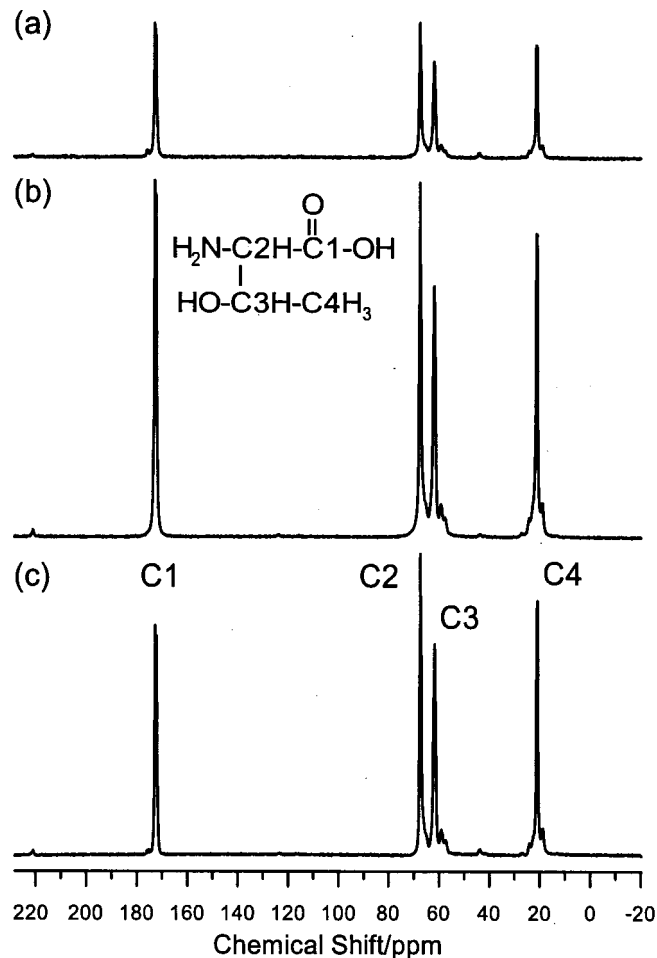


FIG. 1. ^{13}C MAS spectra of uniformly ^{13}C , ^{15}N -labeled L -threonine observed using a ^{13}C 90° pulse without NOP (a) and with NOP (b) and using CP (c). For the ^{13}C pulse experiment without NOP, the relaxation interval was 300 s. For NOP, the NOP time was 10 s. For CP, the relaxation interval was 5 s and the CP contact time was 3.8 ms. 64 FIDs were accumulated for each experiment, and the spectra are plotted on the same amplitude scale and can be directly compared.

tion ($\nu_1 = \nu_{\text{MAS}} = 20$ kHz). For the CP spectrum [Fig. 1(c)], the relaxation interval of 5 s (^1H $T_1 \sim 0.8$ s) and the CP contact time of 3.8 ms were used. Since the repetition time of 300 s for the single 90° pulse experiment [Fig. 1(a)] is much longer than the longest ^{13}C T_1 value (~ 30 s) in Thr, the spectrum ensures the full signal intensities at thermal equilibrium. We then obtained the enhancement factor in NOP (η_{NOP}) and that in CP (η_{CP}); the area intensity of each peak in Figs. 1(b) and 1(c) is expressed in values relative to the corresponding intensity in Fig. 1(a). The obtained enhancement factors in NOP are $\eta_{\text{NOP}} = 2.65, 2.67, 2.66$, and 2.72 for C1 (COOH), C2 (C_α), C3 (C_β), and C4 (CH_3), respectively, which are significantly larger than those in CP: $\eta_{\text{CP}} = 1.52, 1.99, 2.04$, and 2.02 , for C1–C4, respectively. All four ^{13}C signals are almost uniformly enhanced by NOP, but not by CP. The unequal enhancement by CP is attributed mainly to different optimal CP contact times and different ^{13}C spin-lattice relaxation times ($T_{1\rho}^S$) in the rotating frame for different carbons. In fact, it was observed that an optimal CP contact time for C2–C4 is ≈ 0.8 ms, while that for C1 is ≈ 3.8 ms. Even at these optimal contact times for the indi-

vidual carbons, however, we observed unequal η_{CP} values: $C1=1.5$, $C2=2.2$, $C3=2.1$, and $C4=2.4$ (spectra not shown). This fact shows that even if the optimal contact times are equal for all carbons, quantitative comparison of signal intensities are difficult due to different $T_{1\rho}^S$.

The rotational correlation time of the CH_3 group at 300 K is calculated to be $\tau_r=6.1\times 10^{-11}$ s from the activation energy and the pre-exponential factor reported for L-threonine.¹⁸ For this τ_r value, the NOE enhancement factor is calculated from Eq. (2) to be $\eta_{\text{NOE}}\sim 2.9$, which is in agreement with that observed ($\eta_{\text{NOP}}\sim 2.7$) when the reduction indicated in Eq. (8) is taken into account. For example, putting $N=3$ for Thr and $T_1^L=10$ s, $T_1^S=0.25$ s, and $k=1\text{ s}^{-1}$, which were estimated roughly for Thr, into Eq. (8), we have $\eta_{\text{NOP}}\sim 2.8$. Further, the somewhat smaller η_{NOP} for the other carbons ($C1-C3$) can also be explained by Eq. (8) for a finite k value in the intermediate region. The NOP enhancement in Thr is efficient owing to the large NOE due to the short rotational correlation time of the CH_3 group and also owing to the fast $^{13}\text{C}-^{13}\text{C}$ transfer due to the short $^{13}\text{C}-^{13}\text{C}$ distances between the CH_3 carbon and the other three carbon atoms.

Next, we undertook NOP experiments of uniformly ^{13}C , ^{15}N -labeled glycyloisoleucine (Gly-Ile), of which the two carbons of the glycine are far from the two CH_3 carbons of the isoleucine sidechain. Figures 2(a) and 2(b) show the normalized ^{13}C spectra observed for Gly-Ile with a repetition time of 5 s (a) without NOP and (b) with NOP (DARR at $\nu_1=\nu_{\text{MAS}}=20$ kHz), showing that appreciable NOP enhancement occurs uniformly for all eight carbons whose assignment is given in Ref. 13. This shows that the $^{13}\text{C}-^{13}\text{C}$ transfer under DARR is sufficiently fast to distribute the ^{13}C polarization created by NOP for the $^{13}\text{CH}_3$ carbons ($C7, C8$) in the isoleucine sidechain to the other carbons. The enhanced $^{13}\text{C}-^{13}\text{C}$ transfer by DARR irradiation was appreciated further by observing ^{13}C spin-lattice relaxation curves. Figures 3(a) and 3(b) show the ^{13}C spin-lattice relaxation curves of Gly-Ile with (a) and without (b) the DARR irradiation ($\nu_1=\nu_{\text{MAS}}=20$ kHz). The curves observed without DARR [Fig. 3(b)] show that the ^{13}C magnetizations decay with the individual time constants of $\approx 0.1-30$ s. The time constants spread in a wide range demonstrates that the $^{13}\text{C}-^{13}\text{C}$ polarization transfer (spin diffusion) among them is considerably slow. This is brought about by averaging of $^{13}\text{C}-^{13}\text{C}$ dipolar couplings by fast MAS ($\nu_{\text{MAS}}=20$ kHz). Analysis of the ^{13}C T_1 curves to deduce polarization transfer rates would be interesting, however, it is out of the scope of this work, and will be published elsewhere. The curves under DARR [Fig. 3(a)] show that the polarization transfer rates turn significantly higher under DARR, allowing the ^{13}C spins with short T_1 to act as a sink of relaxation. Similar equalization of T_1 by fast spin diffusion is commonly found for ^1H spins in solids,^{19,20} which has been taken as a direct evidence for the legitimacy of the spin-temperature hypothesis. For ^{13}C spins under DARR, however, Fig. 3(a) shows that the $^{13}\text{C}-^{13}\text{C}$ polarization transfer is much enhanced, but is still not fast enough to achieve a common spin temperature within 1–2 s. Nevertheless it occurs nonselectively, indicat-

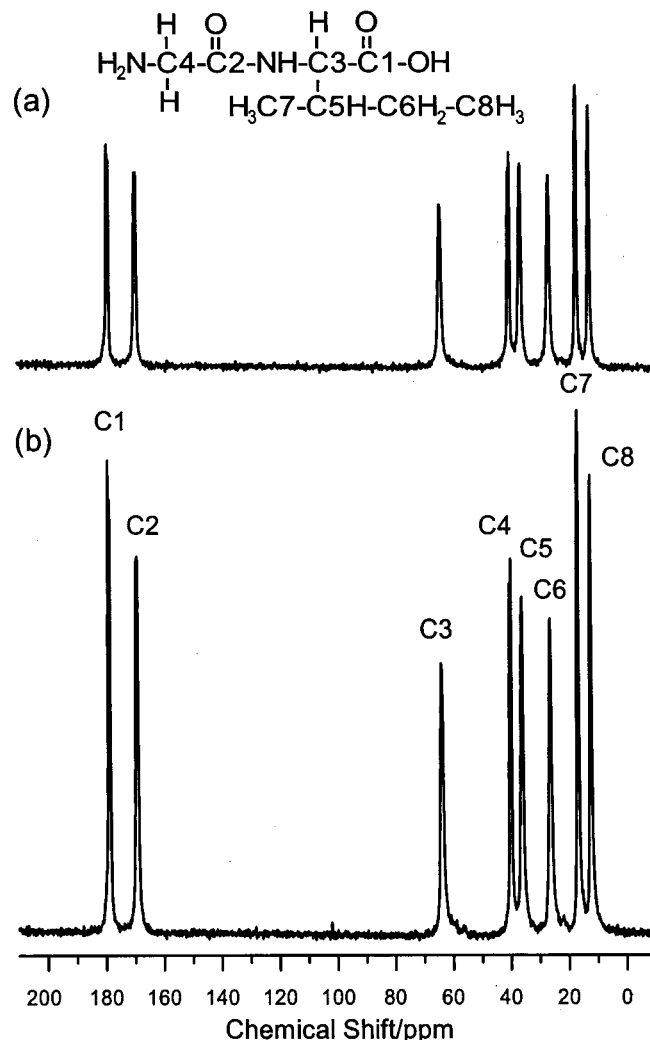


FIG. 2. ^{13}C MAS spectra of uniformly ^{13}C , ^{15}N -labeled glycyloisoleucine observed by a ^{13}C 90° pulse (a) without DARR irradiation and the pulse repetition time of 5 s and (b) with DARR irradiation for 5 s. 64 FIDs were accumulated for each experiment, and the two spectra are plotted on the same amplitude scale and can be directly compared.

ing the capability of distributing the polarization created by NOE in $^{13}\text{CH}_3$ to the other ^{13}C spins.

Figures 4(a) and 4(b) show the NOP-time dependence of the signal area intensities for the eight carbons of Gly-Ile with (a) the ^1H rf-intensity at the DARR condition ($\nu_1=\nu_{\text{MAS}}=20$ kHz) and (b) that at the off-DARR condition of $\nu_1=6$ kHz, which may be enough to cause NOE but $^{13}\text{C}-^{13}\text{C}$ recoupling efficiency is low. The signal intensities for the individual carbons at various NOP times are normalized by the signal intensities observed using a ^{13}C 90° pulse with a repetition time of $300\text{ s} \geq 5T_1$. Hence, the final intensities represent the NOP enhancement factors η_{NOP} for the individual carbons. It was observed that the time required for all carbons other than the two methyl carbons to reach an equilibrated intensity is shorter for the experiment under DARR [Fig. 4(a)] than that under off-DARR irradiation [Fig. 4(b)], which is most apparently appreciated for C2 ($^{13}\text{C}=\text{O}$ of Gly) and C4 ($^{13}\text{CH}_2$ of Gly). The slower equilibration rates observed for them under off-DARR irradiation [Fig. 4(b)] are ascribed to the fact that these two carbons are dis-

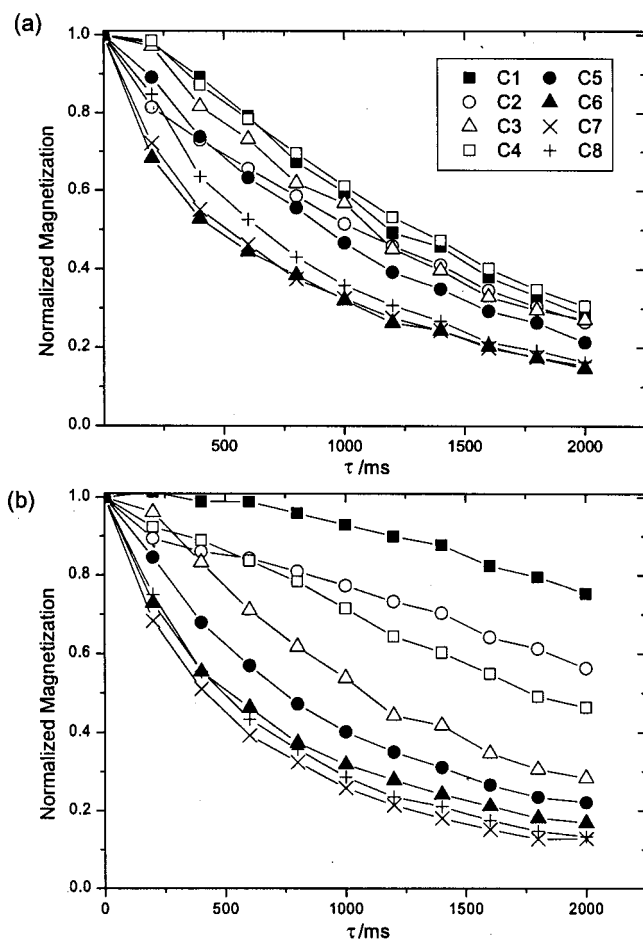


FIG. 3. ^{13}C spin-lattice relaxation curves of uniformly ^{13}C , ^{15}N -labeled glycyllsleucine with (a) and without (b) the DARR irradiation. The Torchia's pulse sequence (Ref. 15) was used under $\nu_{\text{MAS}} = 20$ kHz. The assignment of the ^{13}C signals numbered in Fig. 2(b) is found in Ref. 13. The solid lines are for eye guidance.

tant from either of the two CH_3 carbons (C7 and C8 of Ile).

In Table I, we collate the ^{13}C – ^{13}C distances from the methyl carbons ($r_{\text{C-C7,8}}$), which are calculated from the atomic coordinates determined by an x-ray diffraction study (unpublished). Table I also lists the apparent NOP buildup rates k_{NOP} determined by fitting the observed data to the following single exponential function,

$$S(t)/S_0 = \eta_{\text{NOP}} \{1 - \exp(-k_{\text{NOP}} t)\}, \quad (10)$$

using η_{NOP} and k as fitting parameters. The solid curves in Fig. 4 are the best-fit curves with the parameters listed in Table I. It should also be pointed out here that Eq. (10) is derived from Eq. (6) at the slow polarization transfer limit ($k=0$) with $k_{\text{NOP}} = 1/T_1^S$ under ^1H saturation ($\langle I_Z \rangle = 0$). Due mostly to these simplifying assumptions, the single-exponential fitting does not reproduce the observation particularly at the initial NOP region. We have not tried to fit the observed data by using Eqs. (5)–(7) because of the complexity of the eight ^{13}C spin system.

Enhanced ^{13}C – ^{13}C transfer is evidently observed for C1–C4, k_{NOP} under DARR being larger than that under off-DARR (Table I), but not for C5 and C6. C5 and C6 are

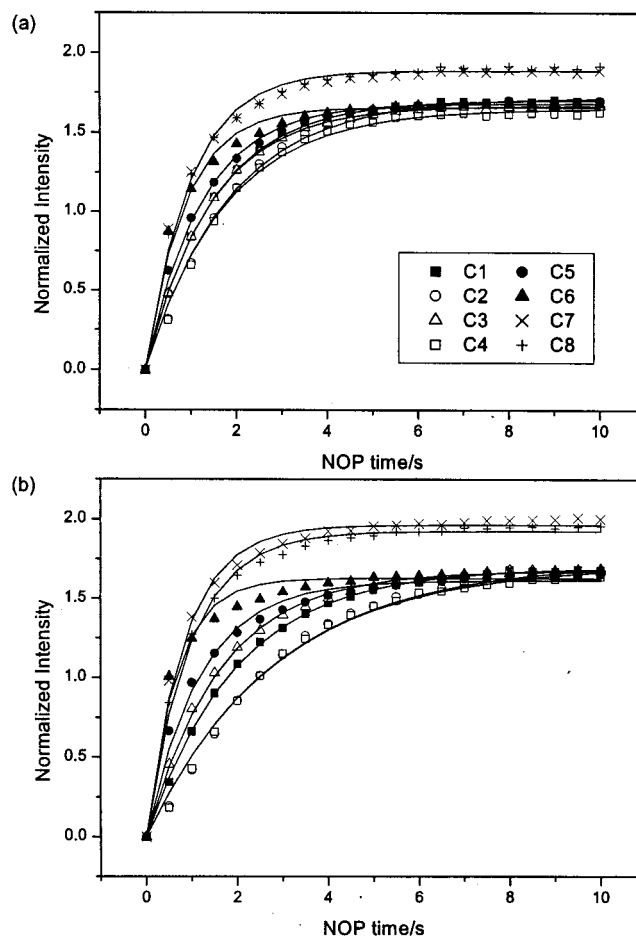


FIG. 4. NOP time dependence of the area intensities of the ^{13}C signals in uniformly ^{13}C , ^{15}N -labeled glycyllsleucine. DARR irradiation ($\nu_1 = \nu_{\text{MAS}} = 20$ kHz) was applied for (a), while $\nu_1 = 5$ kHz for (b). Each signal intensity is given by taking the corresponding area intensity observed by a ^{13}C 90° pulse with a relaxation interval of 300 s as 1.0. The solid lines are the best-fit curves to Eq. (10) with the best-fit parameters collated in Table I.

carbons bonded directly to the methyl carbons, C7 and C8, respectively, and thus direct NOE enhancement from ^1H in the methyl groups would occur in addition to NOP. Hence for C5 and C6, acceleration of k_{NOP} under DARR is not appreciable. For C6 in particular, we found that the C6–C8 bond apparently shows an unusual bond length, which may be caused by a large thermal vibration of C8.¹³ Further, the observed ^{13}C T_1 of C6 is as short as those of the methyl carbons (Fig. 3). Hence for C6, direct NOE from the C(6) H_2 protons as well as NOE due to fluctuation of the C6–C8 dipolar interaction should also contribute to $S(t)$ of C6. Thus omitting C6, we show the correlation between k_{NOP} and $r_{\text{C-C7}}$ in Fig. 5. The observed correlation indicates a possibility of determining internuclear distances roughly by the polarization transfer experiment under DARR, which is currently underway and will be published elsewhere. Here we would like to point out that for $r_{\text{C-C7}} \geq 0.5$ nm intermolecular NOP becomes appreciable, thus leading k_{NOP} being insensitive to $r_{\text{C-C7}}$. Hence for deducing structural information from the polarization transfer experiment under DARR, di-

TABLE I. Best-fit parameters to the NOP-time dependence data in Fig. 4 and the C–C distances from the CH₃ carbons (C7, C8).

	On DARR [Fig. 4(a)]				Off DARR [Fig. 4(b)]				Distance/nm	
	η_{NOP}	σ	$k_{\text{NOP}}/\text{s}^{-1}$	σ	η_{NOP}	σ	$k_{\text{NOP}}/\text{s}^{-1}$	σ	$r_{\text{C-C7}}$	$r_{\text{C-C8}}$
C1	1.704	0.002	0.677	0.004	1.698	0.004	0.500	0.004	0.287	0.496
C2	1.719	0.011	0.546	0.014	1.737	0.022	0.348	0.010	0.496	0.560
C3	1.669	0.002	0.700	0.003	1.678	0.006	0.610	0.010	0.255	0.391
C4	1.650	0.012	0.573	0.017	1.718	0.021	0.353	0.012	0.619	0.639
C5	1.684	0.006	0.814	0.016	1.617	0.012	0.836	0.034	0.145	0.241
C6	1.658	0.012	1.158	0.056	1.630	0.015	1.490	0.105	0.250	0.164
C7	1.846	0.012	1.078	0.038	1.966	0.012	1.173	0.046	0.0	0.289
C8	1.846	0.011	1.078	0.041	1.927	0.009	1.024	0.030	0.289	0.0

lution of the fully ¹³C-labeled sample by a natural abundance one should be used.

Table I shows that the NOP enhancement factors for the two CH₃ carbons ($\eta_{\text{NOP}} \sim 1.9$) are appreciably larger than those of the other carbons ($\eta_{\text{NOP}} \sim 1.7$). Further, the nonmethyl carbons show the same η_{NOP} for the two experiments in spite of the different equilibration rates, while the CH₃ carbons have slightly smaller η_{NOP} under DARR. Putting $N=3$ for Gly-Ile (two methyl carbons and six non-methyl carbons) and $T_1^L=10$ s, $T_1^S=0.25$ s, and $k=1$ s⁻¹, which are estimated roughly from Fig. 3(a), into Eq. (8), we have $\eta_{\text{NOP}}^S \sim 1 + 0.94\xi_{\text{NOE}}$ and $\eta_{\text{NOP}}^L \sim 1 + 0.85\xi_{\text{NOE}}$, which explains qualitatively the observed difference in the apparent enhancement factors for the CH₃ carbons (~ 1.9) and the other carbons (~ 1.7). Further, the observed reduction of η_{NOP}^S of the two CH₃ carbons under DARR can be ascribed to the increase of the polarization transfer rate k due to DARR.

The observed enhancement factors of $\eta_{\text{NOP}} \sim 1.9$ for the two CH₃ carbons (C7 and C8) are significantly smaller than the maximum factor of 2.99. The smaller enhancement would be due partially to the polarization loss by the transfer to the other carbons [Eq. (8)] and mainly to a long CH₃ rotational correlation time not to fulfil the extremely narrow-

ing condition. In fact, Naito *et al.*⁷ successfully reproduced their observed η_{NOE} value of 1.68 for the CH₃ carbon in *L*-alanine by calculation with the literature rotational correlation time τ_r of 1.6×10^{-9} s. Unfortunately the ¹H T_1 curve for *L*-isoleucine has not been fully analyzed. Hence, we estimated τ_r to be $\sim 7 \times 10^{-10}$ from $\eta_{\text{NOE}} \sim 1.9$ using Eq. (2). The τ_r value is comparable to the τ_r values at 300 K for the CH₃ groups in some other amino acids:¹⁸ $\tau_r = 1.2 \times 10^{-9}$ s for *L*-alanine, 1.2×10^{-10} s for *DL*-leucine, 2.5×10^{-11} s for *DL*-norleucine, 6.1×10^{-11} s for *L*-threonine, and 1.8×10^{-10} s for *L*-valine.

Quantitativity of ¹³C intensities is examined by comparing the area intensities observed for Gly-Ile using a ¹³C 90° pulse without NOP (the relaxation interval was 300 s), with NOP (the NOP time was 6 s) and using CP (the CP time was 2.6 ms and the relaxation interval was 4 s). For the 90° pulse experiment without NOP, the observed area intensities for the individual carbons are expressed in values relative to the average area intensity for the eight carbons. They are almost equal to unity with the small standard deviation $\sigma = 0.035$, showing good uniformity for the relaxation interval of 300 s. The observed signal intensities by NOP and CP for the individual carbons were normalized by the corresponding intensities for the 90° pulse experiment and collated in Table II together with the averages and the standard deviations σ . For the 90° pulse experiment with NOP, the standard deviation calculated for the eight carbons is somewhat larger: $\sigma = 0.098$. However, as indicated in Eq. (8), the different enhancement factors for the CH₃ carbons and the other carbons should be taken into account. The average and the standard deviation obtained for the C1–C6 carbons are 1.65 and $\sigma = 0.022$, respectively, showing excellent uniformity achieved by NOP. For the CP spectrum, the standard deviation is the largest ($\sigma = 0.237$), showing that care must be taken to compare the intensities obtained by CP quantitatively. The larger variation found for CP is attributed to the differences of the ¹³C spin-lattice relaxation times in the rotating frame and the CP rates among the carbons.

Figure 6 shows the DARR rf-strength dependence of the signal intensities observed for Gly-Ile with the NOP time of 5 s and $\nu_{\text{MAS}} = 20$ kHz, demonstrating that in the polarization transfer experiment under DARR, a slight misadjustment of the ¹H rf intensity or the spinning frequency from the DARR condition is not crucial; ± 2 kHz misadjustment from the DARR condition ($\nu_1 = \nu_{\text{MAS}} = 20$ kHz) causes only

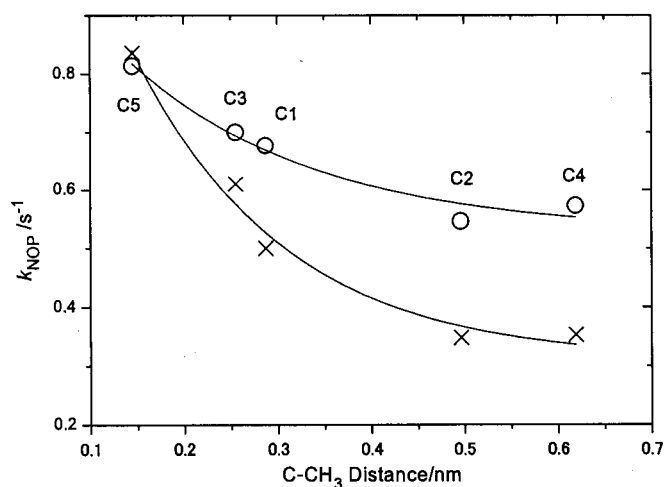


FIG. 5. Correlation between the apparent NOP buildup rate and the C–C distance to the CH₃ carbons (C7) for C1–C5 in uniformly ¹³C, ¹⁵N-labeled glycylisoleucine; open circles denote data under DARR irradiation ($\nu_1 = \nu_{\text{MAS}} = 20$ kHz) and crosses indicate data under off-DARR ($\nu_1 = 6$ kHz). The solid lines are for eye guidance.

TABLE II. Normalized area intensities of the eight carbons of uniformly ^{13}C , ^{15}N -labeled glycylisoleucine.^a

Method	C1	C2	C3	C4	C5	C6	C7	C8	Average	σ
Without NOP	1.03	1.07	0.99	1.01	0.97	0.98	1.00	0.95	1.00	0.035
With NOP	1.67	1.66	1.64	1.61	1.67	1.67	1.87	1.88	1.71	0.098
CP	1.78	1.99	2.02	1.99	2.17	2.29	2.50	2.47	2.15	0.237

^aFor the ^{13}C 90° pulse experiment without NOP (the first row in the table), the area intensity of each carbon signal was expressed in values relative to the average of the area intensities of the eight carbon signals. For the ^{13}C 90° pulse experiment with NOP (the second row in the table) and the CP experiment (the last row in the table), the area intensity for each carbon signal was normalized by the corresponding area intensity in the ^{13}C 90° pulse spectrum without NOP.

a few percent change in intensity. However, the increase of the intensities of the CH_3 carbons (C7, C8) and the decrease of the other intensities particularly the glycine carbons (C2, C4) are notable at rf intensities far from the DARR condition. This tendency can also be confirmed in Fig. 4, and as have pointed out, can be explained by Eq. (8) with a slow polarization transfer rate k at off-DARR conditions.

It would be interesting to examine whether NOP is applicable to natural-abundance samples. Figure 7 shows the ^{13}C MAS spectra observed for nonlabeled dimedone (5,5-dimethyl-1,3-cyclohexanedione) using a ^{13}C 90° pulse without (a),(b) and with NOP (NOP time of 10 s) (c). The relaxation interval without NOP [Fig. 7(b)] was chosen to be 10 s to compare with the NOP spectrum [Fig. 7(c)], and that for the spectrum in Fig. 7(a) was 300 s to obtain a fully relaxed spectrum. The signals C7 and C8 are assigned to the CH_3 carbons,²¹ and their NOP enhancement factors are ≈ 3.0 , reaching the theoretical maximum. Interestingly, we found that the signals for the other rigid carbons (C1–C6), especially for the quarternary carbon (C5), do also show significant enhancement. Two signal enhancement mechanisms can be invoked, namely, direct NOE enhancement of the ^{13}C signals (C1–C6) by the ^1H spins in the two CH_3 groups and the ^{13}C – ^{13}C polarization transfer from the two $^{13}\text{CH}_3$ spins. The large enhancement for C5, which is bonded directly to the two methyl carbons, supports the former mechanism. To ex-

amine the latter, a 90° pulse spectrum was recorded after ^1H irradiation for 10 s with the ^1H rf intensity of 5 kHz (not shown), which is deviated significantly from the DARR condition ($\nu_1 = \nu_{\text{MAS}} = 10$ kHz). We observed slight decreases in the C1–C6 intensities compared to that in Fig. 7(c). This reduction is similar to that observed in Fig. 4, showing that the latter ^{13}C – ^{13}C polarization transfer mechanism takes place even for naturally abundant ^{13}C spins.

V. CONCLUDING REMARKS

We have shown that DARR irradiation causes NOE enhancement of $^{13}\text{CH}_3$ carbon signals and distributes the polar-

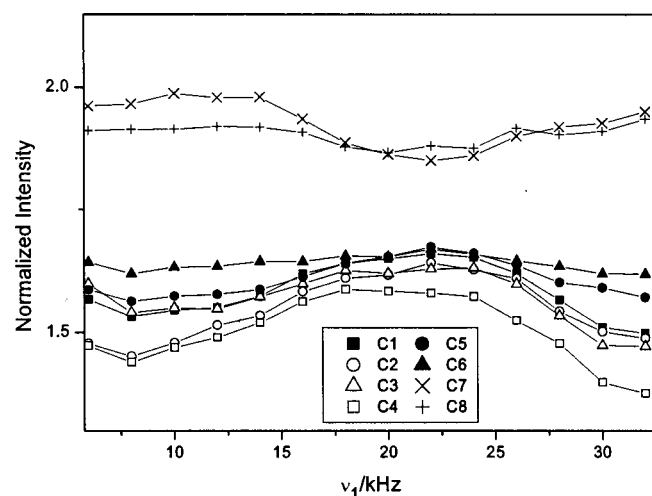


FIG. 6. DARR rf-strength dependence of the intensities of the signals in uniformly ^{13}C , ^{15}N -labeled glycylisoleucine at $\nu_{\text{MAS}} = 20$ kHz. Each signal is normalized to the corresponding area intensity observed by a ^{13}C 90° pulse with a relaxation interval of 300 s. The solid lines are for eye-guidance.

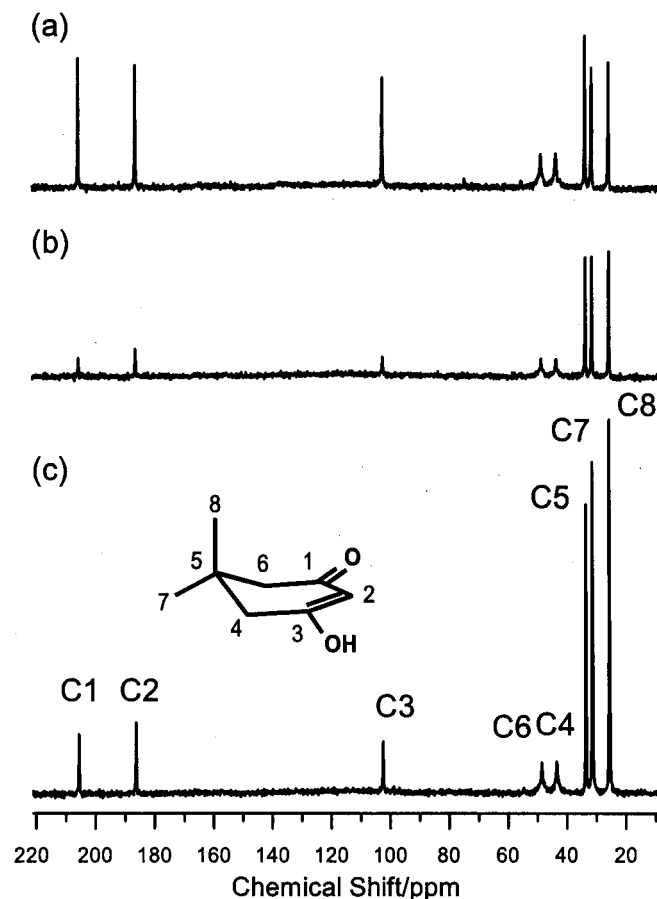


FIG. 7. ^{13}C MAS spectra obtained for nonlabeled dimedone (5,5-dimethyl-1,3-cyclohexanedione) by a ^{13}C 90° pulse without (a),(b) and with NOP (c) under $\nu_{\text{MAS}} = 10$ kHz. The relaxation interval was (a) 300 s and (b) 10 s. For the NOP enhancement (c), ^1H irradiation with $\nu_1 = \nu_{\text{MAS}} = 10$ kHz was applied for 10 s. 256 FIDs were accumulated for each experiment, and the spectra are plotted on the same amplitude scale and can be directly compared.

ization uniformly over all the carbons in a uniformly ¹³C labeled system with mobile parts. Since many amino acids have mobile parts such as the CH₃ groups, the present approach is applicable to most of uniformly/segmentally isotope-labeled peptide samples. Such extensive ¹³C labeling has been becoming an important method for solid NMR to elucidate structural information of biomolecules such as peptides and proteins. For a protein molecule, it is expected that mobility of sidechains would increase due to weaker crystallographical packing force. For example, from the ¹H T₁ data of *Streptomyces subtilisin inhibitor* (SSI),²² we can obtain the correlation time of the motion to be 9.6×10^{-12} s at 300 K, indicating that the extreme narrowing limit of relaxation is achieved thus leading to the maximum NOP enhancement for SSI. Similar results can be deduced for ribonuclease A, α -chymotrypsin, and lysozyme.²³

In uniformly ¹³C labeled peptides, due to the small number ratio of ¹H to ¹³C nuclei, the signal enhancement factor achieved by CP becomes ~ 2.4 , which would practically be reduced because of imperfect spin-locking by phase transient and the effect of finite T_{1ρ} of ¹H and ¹³C. On the other hand, NOP provides the factor of 3 provided that the rotational correlation times of the CH₃ groups are in the extreme narrowing region. NOP enables us to acquire a signal with a short repetition time even if ¹H T₁ is long. For molecules with short T_{1ρ} of ¹H or ¹³C, the CP enhancement becomes smaller, while NOP would work well for such mobile molecules. Furthermore, the present DARR approach is insensitive to rf inhomogeneity and to missetting and fluctuation in ν_{MAS} and H₁, and can easily be carried out with low rf power. Moreover, NOP can be used for quantitative analysis of ¹³C signals in solids, while it is nearly impossible by CP. Lastly, NOP may be used to enhance NMR signals of nuclei with low γ, such as, ⁵⁷Fe, ¹⁰⁷Ag, etc. in a mobile molecule or a molecule having a mobile group, while CP cannot readily be applied because of the necessity of very high rf power in case a certain pulse technique such as TAPF (Ref. 24) is not incorporated.

ACKNOWLEDGMENT

This research was supported by a Grant-in-Aid for Science Research from the Ministry of Education, Culture, Sports, Science, and Technology of Japan.

- ¹S. R. Hartmann and E. L. Hahn, Phys. Rev. **128**, 2042 (1962).
- ²A. Pines, M. G. Gibby, and J. S. Waugh, J. Chem. Phys. **59**, 569 (1973).
- ³A. W. Overhauser, Phys. Rev. **91**, 476 (1953); **92**, 411 (1953).
- ⁴E. G. Paul and D. M. Grant, J. Am. Chem. Soc. **86**, 2977 (1964).
- ⁵F. A. L. Anet and A. J. R. Bourne, J. Am. Chem. Soc. **87**, 5250 (1965).
- ⁶For examples, see, D. T. Okamoto, S. L. Cooper, and T. W. Root, Macromolecules **25**, 3301 (1992); J. L. White and P. Mirau, *ibid.* **26**, 3049 (1993).
- ⁷A. Naito, S. Ganapathy, K. Akasaka, and C. A. McDowell, J. Magn. Reson. **54**, 226 (1983); A. Naito and C. A. McDowell, J. Chem. Phys. **84**, 4181 (1986).
- ⁸K. Takegoshi, S. Nakamura, and T. Terao, Chem. Phys. Lett. **344**, 631 (2001).
- ⁹T. G. Oas, R. G. Griffin, and M. H. Levitt, J. Chem. Phys. **89**, 692 (1988).
- ¹⁰E. R. Andrew, S. Clough, L. F. Farnell, T. D. Gledhill, and I. Roberts, Phys. Lett. **21**, 505 (1966).
- ¹¹D. P. Raleigh, G. S. Harbison, T. G. Neiss, J. E. Roberts, and R. G. Griffin, Chem. Phys. Lett. **138**, 285 (1987).
- ¹²B. H. Meier and W. L. Earl, J. Am. Chem. Soc. **109**, 7939 (1987).
- ¹³K. Nomura, K. Takegoshi, T. Terao, K. Uchida, and M. Kainosho, J. Biomol. NMR **17**, 111 (2000).
- ¹⁴A. E. Bennett, C. M. Rienstra, M. Auger, K. V. Lakshmi, and R. G. Griffin, J. Chem. Phys. **103**, 6951 (1995).
- ¹⁵D. A. Torchia and A. Szabo, J. Magn. Reson. **49**, 107 (1982).
- ¹⁶I. Solomon, Phys. Rev. **99**, 559 (1955).
- ¹⁷A. A. Brooks, J. D. Cutnell, E. O. Stejskal, and V. W. Weiss, J. Chem. Phys. **49**, 1571 (1968).
- ¹⁸E. R. Andrew, W. S. Hinshaw, M. G. Hutchins, and R. O. I. Sjöblom, Mol. Phys. **32**, 795 (1976).
- ¹⁹J. E. Anderson and W. P. Slichter, J. Phys. Chem. **69**, 3099 (1965).
- ²⁰U. Haeblerlen, Philos. Trans. R. Soc. London, Ser. A **299**, 497 (1981).
- ²¹F. Imashiro, S. Maeda, K. Takegoshi, T. Terao, and A. Saika, Chem. Phys. Lett. **92**, 642 (1982).
- ²²K. Akasaka, K. Takegoshi, T. Terao, and S. Ganapathy, Can. J. Chem. **66**, 2014 (1988).
- ²³E. R. Andrew, D. J. Bryant, and E. M. Cashell, Chem. Phys. Lett. **69**, 551 (1980).
- ²⁴K. Takegoshi and C. A. McDowell, J. Magn. Reson. **67**, 356 (1986).